Photonic true-time-delays based on multiplexed substrate-guided wave propagation for phased array antenna applications

Ray T. Chen and Richard L.Q. Li
Microelectronics Research Center
Department of Electrical and Computer Engineering
The University of Texas at Austin, Austin, Texas 78712
Phone:(512)471-4349; Fax:(512)471-8575 Email: raychen@uts.cc.utexas.edu

ABSTRACT

A compact and affordable photonic true-time-delay (TTD) beam steering device for phased array antenna applications using multiplexed substrate-guided wave propagation is presented. The TTD design uses holographic input and output couplers to change the direction of beam propagation as well as optical fanout. Optical delays of various delay lines can be adjusted easily through the substrate thickness and the total internal reflection angle inside the substrate material. Broadband microwave signals for feeding the radiating elements are generated through optical heterodyne technique and they are detected by metal-semiconductor-metal (MSM) detector arrays. The physical aspects of phase-shifters and true-time-delays are first introduced. Then design issues on the photonic TTD architecture and practical constraints on making holographic grating couplers are discussed, especially concerning with recording gratings on DuPont photopolymer materials. Finally, the generation and detection of high frequency microwave signals up to 25 GHz by optical heterodyne techniques are illustrated.

Key words: phased-array-antenna; true-time-delay; holographic couplers, substrate-guided mode propagation; optical heterodyne detection.

1. INTRODUCTION

Phased-array antenna (PAA)s systems combine the signals from as many as thousands of antenna elements to point a directive beam at some angle in space. PAA offers many advantages, including steering without physical movement, accurate beam pointing, increased scan flexibility, precise elemental phase and amplitude control to obtain low spatial sidelobes, and reduced power consumption and weight. The characteristics and angle of the beam are selected electronically across the array elements using analog or digital control of the amplitude and phase of excitation. Such an electronic phase control is traditionally accomplished through bulky, heavy coaxial waveguide feed. Furthermore, as higher frequency phased array operation is pursued, element spacing will become increasingly tight, making waveguide congestion and crosstalk at the array backplane serious concerns. However, innovation and progress in photonic technology are gradually changing the scenario of PAA technology.[1] For instance, photonic systems can be used to provide true-time-delay(TTD) transmission paths for the microwave signals that are distributed to array elements.[2] We will present the distribution of true-time-delay broadband microwave signals for phased array antenna through massive substrate guided waves combined with surface-normal coupling. The broadband microwave signals are generated through optical heterodyne technique. The physical aspects of phase-shifters and true-time-delay are first

0-8194-2233-9/96/$6.00

introduced. Then design issues on the photonic TTD architecture and related topics are addressed. Principle and practical constraints on making holographic grating couplers are discussed next, especially concerning with recording gratings on DuPont photopolymer materials. Finally, the generation and detection of high frequency microwave signals up to 25 GHz by optical heterodyne techniques are illustrated.

2. PHASE SHIFTERS AND TTD CONTROL

For a linear array radiating elements with individual phase control, the far field pattern along the direction of θ_0 can be expressed as

$$E(\theta,t) = \sum_{n=0}^{N} a_n \exp(i\omega_m t)\exp[i(\psi_n + nk_m \Lambda \sin\theta)] \tag{1}$$

where ω_m is the microwave frequency; $k_m = \omega_m / c$ is the wave vector, and Λ is the distance between radiating elements. By electronically controlling the relative phase between successive radiating elements of the array, the direction of the radiated beam can be steered. For example, to point the beam at an angle θ_0, ψ_n is set to the following value

$$\psi_n = -nk_m \Lambda \sin\theta_0. \tag{2}$$

Differentiating the above equation, we have

$$\Delta\theta_0 = -\tan\theta_0 \left(\frac{\Delta\omega_m}{\omega_m} \right). \tag{3}$$

It is clear that for a fixed set of ψ_n's, if the microwave frequency is changed by an amount $\Delta\omega_m$, the radiated beam will drift by an amount $\Delta\theta_0$. This phenomenon is called "beam squint", which leads to an undesirable drop of the antenna gain in the θ_0 direction. To satisfy the wide bandwidth requirements of future PAAs, true-time-delay (TTD) steering techniques must be implemented so that the far field pattern is independent of the microwave frequency. In the TTD approach, the path difference between two radiators is compensated by lengthening the microwave feed to the radiating element with a shorter path to the microwave phase-front. Specifically, the microwave exciting the (n+1) th antenna element is made to propagate through an additional delay line of length $D_n = nL(\theta_0)$. The length of this delay line is designed to provide a time delay

$$t_n(\theta_0) = (n\Lambda \sin\theta_0)/c \tag{4}$$

for the (n+1)th delay element. For all frequencies ω_m, ψ_n is given by

$$\psi_n = -\omega_m t_n(\theta_0). \tag{5}$$

With such a delay set-up, when the second phase term inside Eq. (1) is changed due to frequency "hopping", the first term will change accordingly to compensate for the change such that the sum of the two remain unchanged. Thus, constructive interference can be obtained in the direction θ_0 at all

frequencies. TTDs permit greater bandwidth and hence higher resolution phased array radar operation than what is possible using electronic phase shifters. However, TTDs are not easily realized in practice.[3] For a practical TTD beam steering system, array elements are divided into subarrays and each subarray share a common time delay network. Also, each time-delay unit is also built with discrete time delay increments. The delay selected for each steering angle represents a "quantized" approximation to a linear phase taper that dictates delay times of $0, \Delta t, 2\Delta t, \bullet\bullet\bullet, N\Delta t$ across the array, where Δt is given by $A \sin\theta_0 / c$. In this way, the system provides some, but not all, of the benefits of true-time-delay steering.

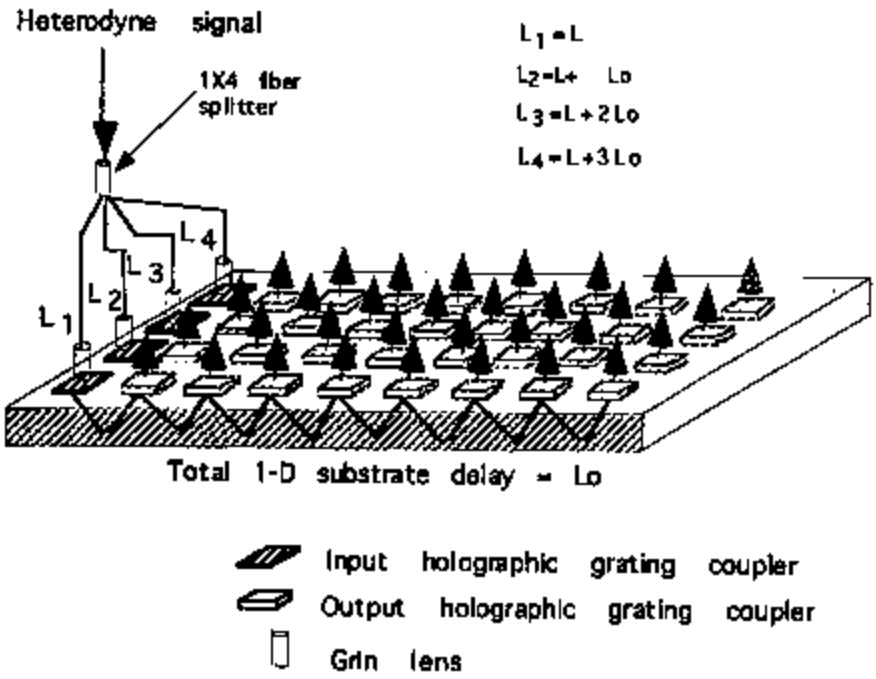

Figure 1 True-time-delay with substrate mode optical fanout

Often times, fiber delay links are used as photonic TTD delay unit.[4] The lengths of the fibers in these links were cut to provide a prespecified set of differential time delays determined by the antenna aperture and its maximum steering angle (θ_{max}). During steering of the phased array, one delay line, as specified by the steering angle, is selected from each of sub-TTD delay module to provide time delay for the antenna subarray fed by the module. In this report, a totally different approach is adopted for the TTDs. Figure 1 illustrates a proposed 2-D substrate mode guided wave optical elements used for massive fan-out true-time-delays with 5-bit resolution.[5] Successive delays of 0, $\Delta\tau$, $2\Delta\tau$, $3\Delta\tau$, ...,$31\Delta\tau$ are provided by substrate-guided wave propagation with different bouncing distances. Optical fanout of various delay lines are accomplished by holographic volume phase grating couplers. These gratings couple the light into and out of substrate modes from the surface-normal direction.

The pivotal issue in this TTD approach lies at constructing highly diffractive efficient input and output holographic couplers on the substrate. Silver halide, dichromated gelatin (DCG) films and photopolymer

holographic recording films can all be used for making holographic couplers. Silver halide suffers from lower resolution and higher scatter. DCG has excellent holographic performance (high index modulation) and low scatter. However, DCG is seriously affected by raw material variability, requires complex wet processing and final holograms must be hermetically sealed to ensure environmental stability.[6] Photopolymer films do not require wet processing and particular means to protect the finished hologram and thus become the material of choice. Volume phase holograms are formed in the photopolymer material (DuPont HRF-600 film) through optical recording which produces a spatial variation in refractive index. The sinusoidal index of refraction variation in the photopolymer material is generated by the diffusion and migration of photosensitive monomers and the subsequent fixing of these monomers. According to Kogelnik's coupled wave theory[7] for thick hologram gratings, the efficiency of a volume transmission grating is a sinusoidal function of the product of grating thickness and index modulation. By selecting the proper thickness for a holographic film with a given index modulation, large than 90% diffraction efficiency has been realized for a desired reconstruction wavelength. Diffraction efficiency can be controlled by varying the photo-exposure dosage or the ratio of the two interference beams.[8]

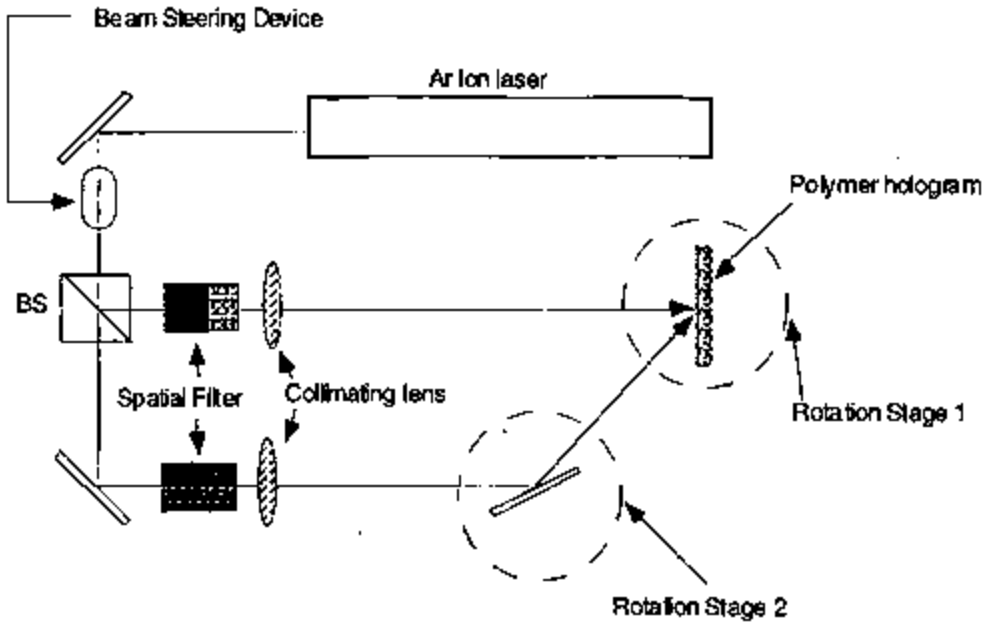

Figure 2 Set-up for making holographic grating couplers

The holographic photopolymer is usually coated from solvent onto a clear support, a 50 μm Mylar® polyester film. A removable cover sheet of 25 μm Mylar film is used to protect the slightly tacky photopolymer. The film is used for holographic recording by removal of the cover sheet and lamination of the film to a glass plate. Hologram recording process consists of exposure, UV cure, and heat processing. A two beam interference recording method for making holographic gratings on photopolymer structures is shown in Fig. 2. The 514 nm line from an Argon ion laser is used as the recording wavelength. The laser output is first split into two separate beams, which are spatially filtered and collimated respectively. These two beams intersect on the photopolymer film with specific designed angles. These angles determine the grating periodicity and the slant angle with respect to the surface normal of the film. The substrate bouncing angle and the diffraction efficiency depend critically on these

two angles. Both types of hologram gratings are created by successively exposing holographic patterns within the selectively defined and sensitized regions of the polymer film.

Design of holographic gratings is accomplished by constructing a grating vector such that a specific phase matching condition can be met. Notice that a particular design is for operation at a specific Bragg diffraction angle and a specific display wavelength. To form a slanted grating coupler which converts a vertical incident wave to a TIR with bouncing angle α in the substrate, the two incident angles of the recording beam with respect to the surface normal of the film are[9]

$$\theta_1 = \sin^{-1}\left\{\frac{n}{n_r}\sin\left[\frac{\alpha}{2} + \sin^{-1}\left(\frac{\lambda_b}{\lambda_r}\sin\left(\frac{\alpha}{2}\right)\right)\right]\right\},$$

and (6)

$$\theta_2 = \sin^{-1}\left\{\frac{n}{n_r}\sin\left[\frac{\alpha}{2} - \sin^{-1}\left(\frac{\lambda_b}{\lambda_r}\sin\left(\frac{\alpha}{2}\right)\right)\right]\right\};$$

where n is the average refractive index of the holographic material, n_r is the refractive index of the medium on top of the holographic emulsion (n_r=1 for air), λ_b and λ_r represent the wavelengths of the recording and display (reconstruction) waves, respectively.

Due to the slanted nature of the grating and to the difference in refractive index between the polymer film and the medium above it, the range of α is limited. To increase α, i.e., increase the bouncing distance of the substrate mode, we can either decrease the ratio of λ_b/λ_r by changing the recording and reconstruction wavelength to increase n_r by putting a high index prism right in front of the holographic emulsion area during recording.

5. PRELIMINARY RESULTS

Figure 3 shows the CCD image of the TTD fanouts with a preliminary one-dimensional TTD test unit. The gradual decrease in fanout intensity is clearly observable. This is caused by the cascading effect of light propagation down the substrate while the output couplers have more or less the same diffraction efficiency. For a practical device, it is desired that the light coupled out surface normally to be uniform in intensity. An uniform light intensity will relax the responsivity requirements for wideband fast MSM detectors, hence achieving a more balanced signal-to-noise ratio at the microwave end. This is critical since signal strength at multigigaherz range is stringently restricted by S/N ratio requirement, wideband amplifier dynamic range and limited detector responsivities. To ensure that the fanout optical signals from each output coupler are uniform in intensity, it is necessary to fine tune the diffraction efficiency from each output couplers.

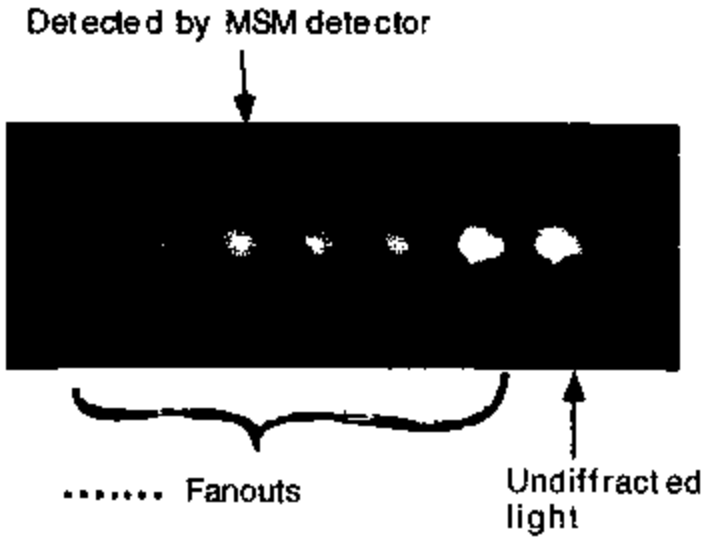

Figure 3. CCD image of TTD fanouts at various substrate mode locations

With the coherent mixing of two CW lasers oscillating at single longitudinal frequencies, microwave frequency rf signals can be generated by optical heterodyne techniques. We employed two tunable diode lasers with a lasing wavelength around 786 nm, which are stabilized by the current and temperature controllers. The line width of the laser is around 100 KHz. As indicated in Fig. 6, the outputs of the lasers are combined by a 50:50 beam splitter, passing an optical isolator and then coupled into the TTD unit at normal incidence. One of the weak fanouts is coupled to a multimode fiber (MMF) with a 10 X microscope objective lens. The output of the fiber is launched directly to an ultrafast photodetector with 60 GHz bandwidth through the matched FC connector. The PD output is amplified through a broadband amplifier and immediately connected to a spectrum analyzer for display. The photocurrent output from the PD contains a DC part and an AC part corresponding to the high frequency rf beat signal. If the optical fields of two separate lasers are given by $E_1 = A_1 \exp(j\omega t)$ and $E_2 = A_2 \exp\{j(\omega + \omega_{12})t\}$, where ω_{12} is the beat frequency and the two lasers are linearly polarized in the same direction. The output of the photodetector in the form of photocurrent is therefore given by [10]

$$i_p(t) = \frac{e\eta}{h\nu}(A_1^2 + A_2^2 + 2F(\omega_{12})A_1A_2\cos(\omega_{12}t)). \tag{7}$$

Here, e is the electron charge, η is the quantum efficiency of the detector, $h\nu$ is the incoming photon energy and $F(\omega_{12})$ is the frequency response function of the PD. The optical-to-electrical conversion represented by Eq.(7) is equivalent to that of directly modulating a laser diode.

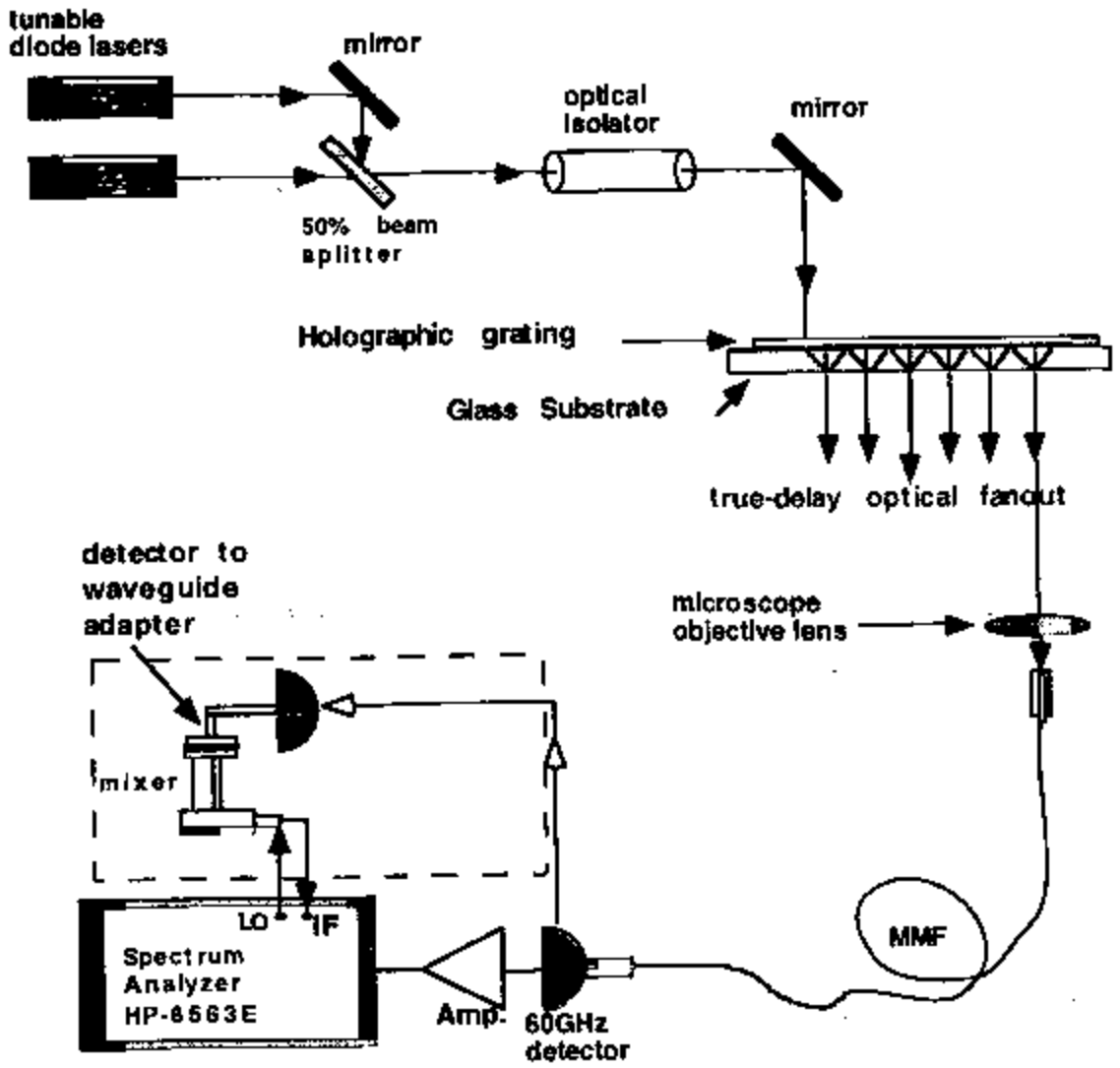

Figure 4. Set-up of the generation of microwave signals by optical heterodyne detection.

With the set-up of Fig. 4, we have successfully produced and detected microwave frequency signals up to the 25.6 GHz band. Figure 5 shows the detected 20 GHz rf signal of one of the fanouts by a spectrum analyzer. A signal to noise (S/N) ratio of ~ 20 dB is obtained. Presently, 25 GHz is limited only by the frequency response of the amplifier and the spectrum analyzer used. Realizing the fact that a small tune of the laser wavelength (a few A°) will provide a large beat frequency, the task of generating wideband rf signals is relatively easy. In fact, microwave signals as high as several hundred gigahertz has already been achieved, only hindered by the difficulties of detecting and demonstrating of such signals. By using external mixers and wideband amplifier, much higher upper frequency [11] is expected.

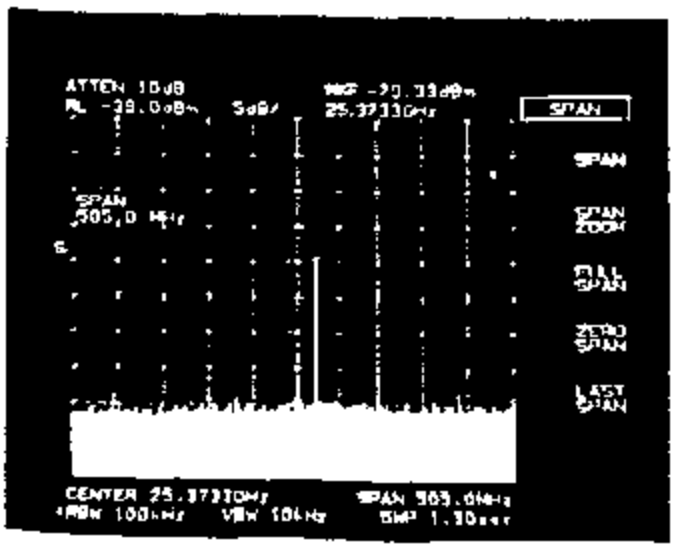

Figure 5 25 GHz Optical heterodyne signal detected by spectrum analyzer

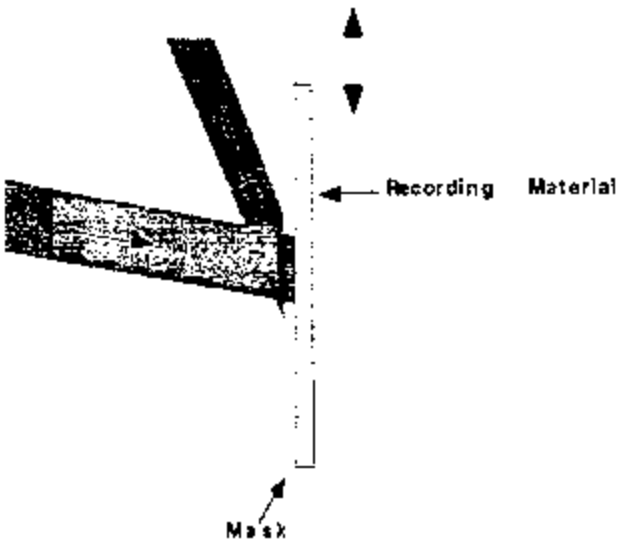

Figure 6 Using masking to implement the diffraction efficiencies of output couplers

To achieve an uniform TTD delay line fanout in intensity, we anticipated by using masking scheme during holographic recording, as illustrated in Fig. 6. Problems related with this method include masking opening size and the influence of multiple exposure on the integrity of the whole hologram. The mask size is affected by the slanted nature of the hologram and the relative small spatial separation

between fanouts. Precise translation stages are required for the successful implementation of this method. This work is currently in progress.

8. ACKNOWLEDGMENTS

This research is supported by the Office of Naval Research. The authors thank Dr. Y. S. Park for his encouragement. Technical discussions with Dr. W. Ng of Hughes Research Lab is also acknowledged.

REFERENCES

[1] H. Zmuda and E.N. Toughlian, "Photonic Aspect of Modern Radar", Artech House, 1994

[2] E. Ackerman, et al., *IEEE MTT-S Digest*, **R-6**, 681(1992).

[3] R.T. Chen and Richard Lee, *SPIE's International Technical Working Group Newsletter* **7**, 1, 8 (May, 1996).

[4] W. Ng, et al., *IEEE J. of Lightwave Technology*, **9**, 1124(1991).

[5] R.T. Chen and R. Lee, *SPIE Technical Digest*, **2689**, 25 (1996).

[6] R. T. Chen, *Optics and Laser Technology.*, **25**, 347-365(1993).

[7] H. Kogelnik, *The Bell System Technical Journal.*, **48**, 2909(1969).

[8] U. Rhee, et al., *Opt. Eng.*, **32**, 1839(1993).

[9] R. T. Chen, S. Tang, et al. *Appl. Phys. Lett.*, **63**, 1883(1993).

[10] S. Kawanish, A. Takada, and M. Saruwatari, *IEEE J. of Lightwave Technology*, **7**, 1, 92(1989).

[11] R.T. Chen, H. Lu, D. Robinson, Z. Sun, and T. Jannson, *Applied Physics Letters*, **60**, 5, 536(1992).